

Sublattice magnetism in σ -phase $\text{Fe}_{100-x}\text{V}_x$ ($x=34.4, 39.9, \text{ and } 47.9$) studied via zero-field ^{51}V NMR

Stanislaw M. Dubiel,^{1,*} José Roberto Tozoni,² Jakub Cieřlak,¹ Daniel Cesar Braz,²
Edson Luiz Gea Vidoto,² and Tito José Bonagamba²

¹*Faculty of Physics and Computer Science, AGH University of Science and Technology, PL-30-059 Kraków, Poland*

²*Instituto de Física de São Carlos, Universidade de São Paulo, Caixa Postal 369, São Carlos 13560-970, SP, Brazil*

(Received 25 June 2009; revised manuscript received 15 January 2010; published 7 May 2010)

The successful measurements of a sublattice magnetism with ^{51}V NMR techniques in the sigma-phase $\text{Fe}_{100-x}\text{V}_x$ alloys with $x=34.4, 39.9, \text{ and } 47.9$ are reported. Vanadium atoms, which were revealed to be present on all five crystallographic sites, are found to be under the action of the hyperfine magnetic fields produced by the neighboring Fe atoms, which allow the observation of ^{51}V NMR signals. Their nuclear magnetic properties are characteristic of a given site, which strongly depend on the composition. Site A exhibits the strongest magnetism while site D is the weakest. The estimated average magnetic moment per V atom decreases from $0.36\mu_B$ for $x=34.4$ to $0.20\mu_B$ for $x=47.9$. The magnetism revealed at V atoms is linearly correlated with the magnetic moment of Fe atoms, which implies that the former is induced by the latter.

DOI: [10.1103/PhysRevB.81.184407](https://doi.org/10.1103/PhysRevB.81.184407)

PACS number(s): 75.50.Bb, 76.60.-k

I. INTRODUCTION

A sigma phase can be produced by a solid-state reaction in some alloy systems in which at least one constituent is a transition element. It has a tetragonal crystallographic structure and its unit cell contains 30 atoms that are distributed over five different crystallographic sites A, B, C, D, and E. Because of the high coordination numbers (12–15), the phase belongs to a family of the so-called Frank-Kasper phases. Among about 50 binary alloys in which the sigma phase was found, only that in the Fe-Cr and Fe-V alloys has well-evidenced magnetic properties.^{1–6} Although magnetic investigations on the sigma phase have been carried since 40 years,^{2,3} its magnetism, which, due to low values of the Curie temperature and of the magnetic moment, is usually termed as weak and low temperature, is not well understood yet. Some features like a lack of saturation of magnetization even in an external magnetic field of 15 T (Refs. 4–6) and the Rhodes-Wohlfarth criterion speak in favor of its itinerant character but it remains fully unknown (a) if both kinds of the constituting atoms contribute to the magnetism, (b) what are the values of the magnetic moments localized at the constituting atoms occupying different crystallographic sites, and (c) is the magnetic structure colinear or not. The difficulty in answering these questions arises on one hand from a failure to produce a big enough single crystal of the sigma phase that could be used in a neutron-diffraction experiment to decipher the magnetic structure, and on the other, in a lack of high-enough resolution of the Mössbauer Spectroscopy, which partly follows from the weak magnetism of the sigma phase and partly from its complex crystallographic structure combined with a chemical disorder of atom distribution over the five sites.⁷

In this paper, we report on a successful measurement of the nuclear-magnetic-resonance (NMR) spectra without applying external magnetic field (so-called zero-field NMR) (Refs. 8–12) on the σ -phase $\text{Fe}_{100-x}\text{V}_x$ samples with $x=34.4, 39.9, \text{ and } 47.9$, which gives a clear evidence that V atoms occupy five sites and have a nonzero spin density (transferred Fe hyperfine magnetic field) that is characteristic of a given site.

II. EXPERIMENTAL

The samples of the σ phase used in this study were prepared by an isothermal annealing of master ingots of the α phase at 973 K for 25 days. More detailed description of the fabrication process and the verification of the final phase and its chemical composition are given elsewhere.⁶ For NMR measurements, the samples were in form of powder (~ 100 mg) obtained by attrition bulk samples in an agate mortar and, afterward, mixed with paraffin.

The zero-field NMR experiments were carried out using a Discovery Tecmag Console, which operates in the frequency range of 1–600 MHz. The spectra were obtained by exciting the nuclei frequency-by-frequency (0.3125 MHz step), within a frequency range of 10–100 MHz, and measuring the respective modules of the complex echo signals acquired.

For the samples $\text{Fe}_{65.6}\text{V}_{34.4}$ and $\text{Fe}_{60.1}\text{V}_{39.9}$, the echoes were obtained after the application of two $1\ \mu\text{s}$ radio-frequency (rf) pulses, separated by a fixed delay of $20\ \mu\text{s}$. The repetition time for the spin-echo experiments was set to 50 ms and the number of averages to 500 scans. However, for the sample $\text{Fe}_{52.1}\text{V}_{47.9}$, due to the low signal-to-noise ratio, the echoes were obtained after the application of two $2\ \mu\text{s}$ radio-frequency pulses, the interpulse delay was set to $7\ \mu\text{s}$, the repetition time to 10 ms, and the number of averages to 150 000 scans. All the measurements were carried out at 4.2 K.

III. RESULTS AND DISCUSSION

The NMR signal can in this case originate from both ^{51}V and ^{57}Fe nuclei. However, the main lines observed in the spectra (Figs. 1 and 2) were assigned to the ^{51}V nuclei due to the following three main reasons: (i) much higher natural abundance of the ^{51}V nuclei (99.8%) as compared to that of ^{57}Fe (2.2%); (ii) more intense gyromagnetic factor of ^{51}V nuclei (11.2 MHz/T) in contrast with that of ^{57}Fe (1.4 MHz/T); and (iii) Mössbauer experiments carried out for similar samples to those studied in this work indicate that local hyperfine magnetic fields on the Fe sites are dispersed from 5 to

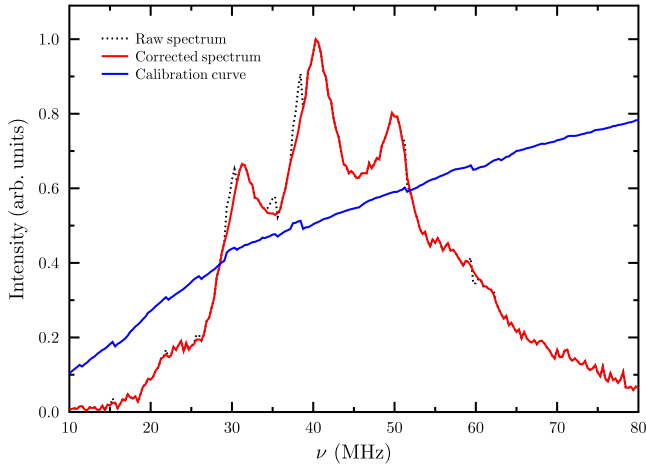


FIG. 1. (Color online) Raw ^{51}V NMR spectrum observed for the sample $\text{Fe}_{65.6}\text{V}_{34.4}$ together with a calibration curve and corrected spectrum.

20 T at 4.2 K, with an average value of about 13 T.⁶ Taking into consideration the two last reasons, one would expect to observe ^{57}Fe lines in the NMR spectrum in the frequency range of 5–30 MHz while the recorded spectra are observed from 10 to 100 MHz. Consequently, one could conclude that all the observed lines are associated with ^{51}V nuclei, which have spin 7/2. Additionally, preliminary NMR measurements performed at the center of each peak (A through E) of the spectrum observed for sample $\text{Fe}_{65.6}\text{V}_{34.4}$ indicated that they present quadrupolar oscillations, a specific behavior of quadrupolar nuclei. In our case, only ^{51}V nuclei are quadrupolar.⁹ As a result, the widths, positions, and shapes of the spectral lines associated to these nuclei should be affected by both hyperfine magnetic fields and electric quadrupolar interactions of each ^{51}V site, being these contributions on the order of units to tens of megahertz and about 300 kHz, respectively. All the spectra shown below were processed using the procedures described in Ref. 10, using the spin-echo integral method to reconstruct them.

Due to the fact that the NMR spectrometer was used for detecting very wide spectra, special care was taken to avoid

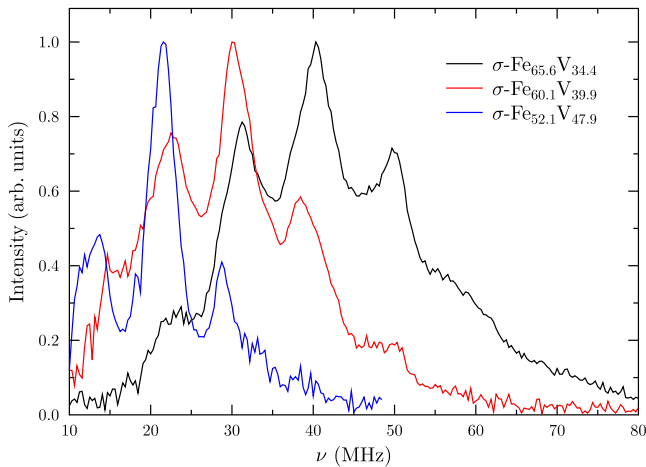


FIG. 2. (Color online) ^{51}V NMR corrected spectra recorded at 4.2 K for samples with Fe contents $(1-x)$ equal to 65.6, 60.1, and 52.1, in sequence from right to left.

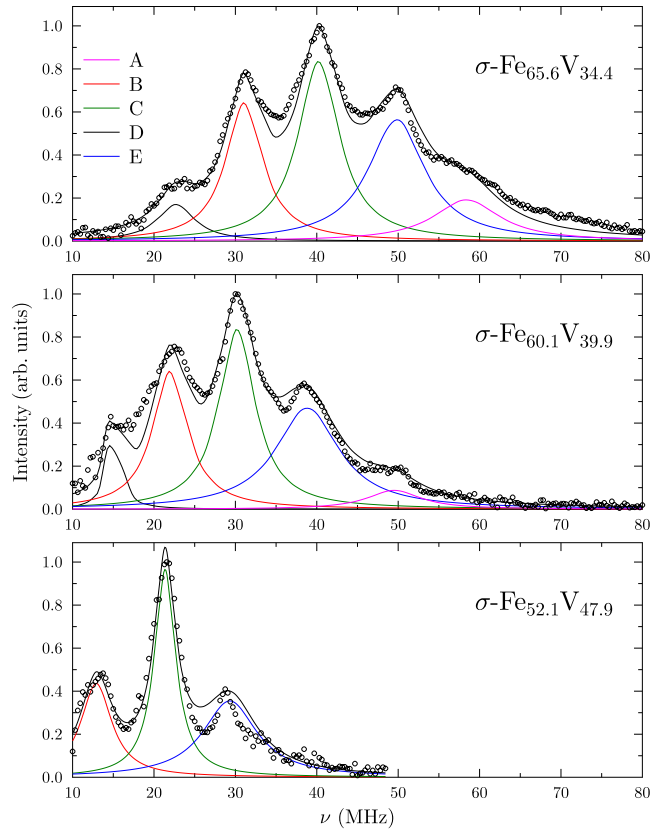


FIG. 3. (Color online) Corrected (circles) and deconvoluted ^{51}V NMR spectra (full lines) recorded at 4.2 K for the investigated samples.

spurious artifacts affecting the wide line spectral shape from transmitter, receiver, cables, rf probe, etc. In order to circumvent all the undesirable contributions, the radio-frequency probe coil was designed to avoid self-resonances in the experiment frequency range (10–100 MHz) and its connections to the spectrometer were made without using tuning/matching by capacitors and transmitter/receiver duplexing with quarter-wavelength cable. Before the experiments, the following calibration procedures were carried out: (i) the rf probe was fully characterized by the use of a vector impedance meter; (ii) the spectrometer frequency response, without probe, was analyzed by connecting the transmitter directly to the receiver and running the experiment over the full experiment frequency range; and (iii) the same procedure used in (ii) was repeated with the inclusion of the rf probe. After these procedures, it was possible to observe all the spurious contributions of the spectrometer to the spectra, allowing to safely eliminate them from the observed spectra. Figure 1 shows the raw spectrum observed for the sample $\text{Fe}_{65.6}\text{V}_{34.4}$ together with the most representative calibration curve, where one can easily observe the spurious artifacts introduced by all the components of the spectrometer. After quickly identifying the spurious peaks, they were simply removed from the spectrum by extracting the corresponding points from the spectrum data, without any additional data manipulation. In the cases where the signal to noise was not good enough to distinguish the signal from the noise for both calibration curve and NMR data, the spectrum intensity was kept the same.

TABLE I. Best-fit parameters as obtained for ^{51}V spectra recorded at 4.2 K on the investigated samples.

Site	Line position (MHz)			Line separation ^a (MHz)		
	$x=34.4$	$x=39.9$	$x=47.9$	$x=34.4$	$x=39.9$	$x=47.9$
D	22.70	15.10				
B	31.10	22.00	12.91	8.40	6.90	
C	40.25	30.20	21.36	9.15	8.20	8.45
E	49.80	38.83	29.32	9.55	8.63	7.96
A	58.40	49.50		8.60	10.67	
Average line separation (MHz)				8.93	8.60	8.20
Average frequency (MHz)				42.12	31.11	22.07

^aFrequency shift between two neighboring lines.

In order to get the final shape for the spectra, the intensities were corrected to compensate the frequency-dependent sensitivity of the NMR system, which was also experimentally estimated. Figure 2 shows the final spectra for all three samples, taking the same procedures discussed above to ensure that the spectral features are predominately due to the ^{51}V hyperfine interactions. As discussed before, the widths, positions, and shapes of the spectral lines associated to these nuclei should be affected by both hyperfine magnetic fields and electric quadrupolar interactions for each ^{51}V site. Considering that ^{51}V nuclei have spin $7/2$, one should expect to observe seven lines equally separated by the quadrupolar coupling, which was estimated to be about 300 kHz. This feature is not observed for all the spectra measured, indicating that the broad shapes observed for sites A through E are due to superimposed distributions of electric quadrupolar couplings and hyperfine magnetic fields, being the last interaction more important for the large broadening observed since quadrupolar couplings would not account for the large linewidths detected.

With the purpose of estimating the area of each line of the spectra, they were decomposed by a multiple Lorentzian fitting procedure, using 5, 5, and 3 peaks for samples $\text{Fe}_{65.6}\text{V}_{34.4}$, $\text{Fe}_{60.1}\text{V}_{39.9}$, and $\text{Fe}_{52.1}\text{V}_{47.9}$, respectively (see Fig. 3), assuming they should consist basically of five resonance lines corresponding to the different crystallographic sites A, B, C, D, and E, superimposed on a background. In the sample with the highest content of vanadium, we observed only three lines because of the very low signal to noise for this NMR measurement, due to the lower hyperfine magnetic field, not allowing the observation of the lines A and D.

All the fitting parameters were kept free to fit the line shapes during the spectral decomposition procedures, though the correlations among the line intensities (areas) and the respective site populations obtained from neutron diffraction⁷ were taken into account. Due to this reason, errors of about 10% for the line intensities (areas), which include, not only the error indicated by the fittings but also the linewidth variability should be noticed. The shoulder observed in the higher-frequency side of the $\text{Fe}_{65.6}\text{V}_{34.4}$ sample's spectrum (line A), which was associated to spurious signals, and neglected in the fitting procedures, disappears

for the other samples or eventually hides under the line A. In this case, mostly for the sample $\text{Fe}_{60.1}\text{V}_{39.9}$, this could give an additional error to the line A intensity (about 20%) since only five peaks were considered in the fitting procedure.

The best-fit parameters obtained with the above-described procedure are given in Table I. Taking in consideration the line intensities and the respective site populations obtained from the neutron diffraction,⁷ one can obtain a good correlation between the two experimental methods, as indicated by the correlation coefficient R^2 in Table II.

Additional correlations were found for the NMR line positions and the magnetic moment per Fe atom versus the Fe content as shown in Figs. 2, 4, and 5, confirming that the bigger the iron concentration, the higher the local magnetic field in the V sites.

Before a more detailed discussion of the results will proceed, let us first notice that a well-defined five-line structure seen in the intensity of the measured spectra is the characteristic feature. This means that (1) the transferred Fe hyperfine magnetic field (spin density) exists on V atoms occupying all five crystallographic sites and (2) it is characteristic of a given site. This agrees, at least, qualitatively with the observation and calculation known for disordered α -Fe-V al-

TABLE II. Relative probabilities, P , of finding V atoms at different sites A, B, C, D, and E in a unit cell of the σ -phase samples of $\text{Fe}_{100-x}\text{V}_x$ compounds as derived from the measured ^{51}V NMR spectra and those, in brackets, obtained from neutron-diffraction studies (Ref. 7). The linear correlation coefficient between the two series of P is denoted as R^2 .

Site	$x=34.4$	$x=39.9$	$x=47.9$
	P (%)	P (%)	P (%)
A	5.8 (0.6)	5.5 (0.8)	-(1.0)
B	21.8 (26.0)	24.3 (24.7)	25.6 (23.3)
C	31.5 (35.1)	33.0 (36.3)	38.4 (36.8)
E	29.2 (36.5)	32.1 (36.3)	36.0 (36.8)
D	11.7 (1.8)	5.1 (1.9)	-(2.1)
R^2	0.86	0.96	0.95

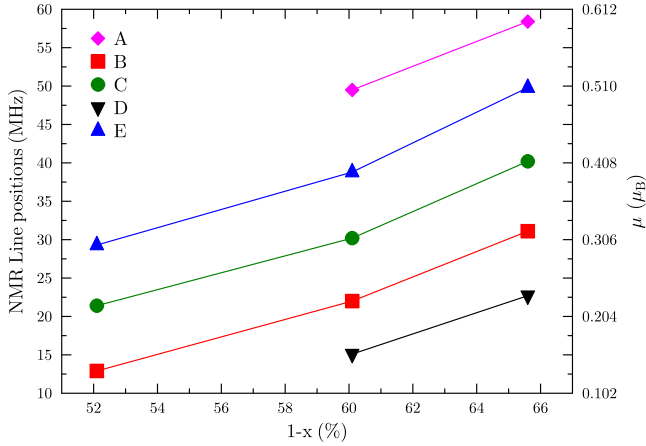


FIG. 4. (Color online) ^{51}V NMR line positions observed for different lattice sites versus Fe content, $(1-x)$. The data are connected to guide the eyes. The right-hand-side y axis has been scaled in the corresponding magnetic moment estimated using the scaling factor as given elsewhere (Refs. 13 and 14).

loys, where V atoms in Fe-rich alloys have magnetic moments on the order of $1\mu_B$.¹³⁻¹⁵

Let us first discuss the question of the effect of composition on the peak position of each of the five resonance lines. As shown in Fig. 2, all three spectra are shifted with $(1-x)$ toward higher frequencies (hyperfine magnetic fields). Concerning positions of particular resonance lines, a strong quasilinear increase with Fe content, $(1-x)$, can be observed for all five sites—see Fig. 4. The increase, which is slightly enhanced for higher Fe concentrations, is rather site independent. The average shift between the subsequent resonance lines has the following approximate values: 8.93 MHz or 0.80 T for $x=34.4$; 8.60 MHz or 0.77 T for $x=39.9$ and, finally, 8.20 MHz or 0.73 T for $x=47.9$. These figures can be rescaled into the underlying magnetic moments. For that purpose, the scaling constant of $9\text{ T}/\mu_B$ deduced from the data published elsewhere^{13,14} can be used. By doing so, the following shifts expressed in Bohr magneton have been obtained: 0.0885 for $x=34.4$, 0.0883 for $x=39.9$, and 0.0813 for $x=47.9$, i.e., they hardly depend on composition. In order to compare this behavior with that of the average magnetic moment per Fe atom, $\langle\mu\rangle$, as determined elsewhere,⁶ a weighted average frequency (gravity center), $\langle\nu\rangle$, of each spectrum was calculated and the relationship between them and Fe contents is displayed in Fig. 5. As can be here seen, both $\langle\nu\rangle$ and $\langle\mu\rangle$ are linearly dependent on $(1-x)$, indicating that the hyperfine magnetic field (spin density) revealed at ^{51}V nuclei has been induced by magnetic Fe atoms. This observation is consistent with the itinerant character of magnetism of the σ -FeV alloys.

IV. SUMMARY

In summary, we have succeeded to record the NMR spectra on magnetic σ -phase samples of Fe-V alloys. The spectra

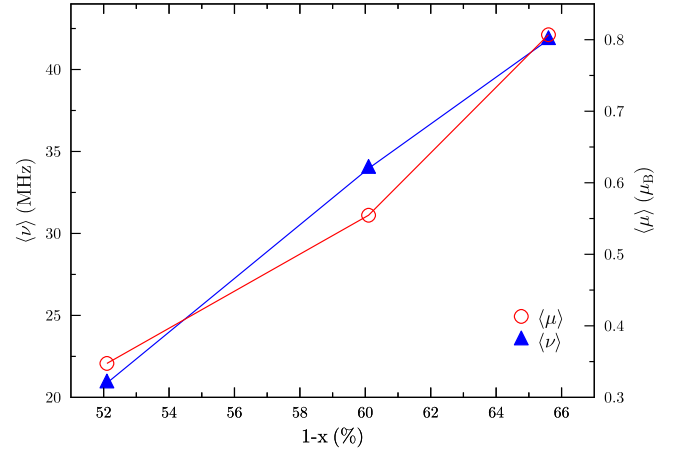


FIG. 5. (Color online) Relationship between the average resonance frequency, $\langle\nu\rangle$, of the measured NMR spectra, the average magnetic moment per Fe atom, $\langle\mu\rangle$, and Fe content, $(1-x)$. The lines connecting the data are drawn to guide the eyes.

give a clear evidence that V atoms occupy all five sublattices and all of them have nonzero hyperfine magnetic fields, hence magnetic moments. The value of the latter strongly depends on the site, and for a given site on the sample composition. The A sites exhibit the strongest magnetism, with a transferred Fe hyperfine magnetic field of 5.21 T ($0.58\mu_B$) for $x=34.4$ and 4.42 T ($0.49\mu_B$) for $x=39.9$ while the D sites are magnetically the weakest ones, having transferred Fe hyperfine magnetic fields (magnetic moment) of 2.03 T ($0.225\mu_B$) for $x=34.4$ and 1.35 T ($0.15\mu_B$) for $x=39.9$. The resonance lines due to these two sites have been not detected for the sample with the highest V content. The average transferred Fe hyperfine magnetic field (magnetic moment) at ^{51}V nucleus decreases from $\langle B\rangle=3.76$ ($0.42\mu_B$) for $x=34.4$ to 1.97 T ($0.22\mu_B$) for $x=47.9$. It is clear from these data and the linear correlation between $\langle\nu\rangle$ and $\langle\mu\rangle$, that the magnetism observed on V atoms strongly depends on the sample composition and it is induced by that of Fe atoms.

Additional ^{57}Fe -enriched samples and experiments are now being prepared in order to measure signals from ^{57}Fe nuclei and quadrupolar oscillations⁹ for all the five ^{51}V sites, which will give additional important structural information about these materials from the NMR point of view.

ACKNOWLEDGMENTS

Authors acknowledge Jair C. C. de Freitas for the discussions about this study. The project was partly supported by the Ministry of Science and Higher Education, Warsaw and the Brazilian Science Foundations FAPESP, CAPES, and CNPq.

*Corresponding author; dubiel@novell.ftj.agh.edu.pl

¹E. O. Hall and S. H. Algie, *Metall. Rev.* **11**, 61 (1966).

²D. A. Read and E. H. Thomas, *IEEE Trans. Magn.* **2**, 415 (1966).

³D. A. Read, E. H. Thomas, and J. B. Forsythe, *J. Phys. Chem. Solids* **29**, 1569 (1968).

⁴J. Cieślak, M. Reissner, W. Steiner, and S. M. Dubiel, *J. Magn. Magn. Mater.* **272-276**, 534 (2004).

⁵J. Cieślak, M. Reissner, W. Steiner, and S. M. Dubiel, *Phys. Status Solidi A* **205**, 1794 (2008).

⁶J. Cieślak, B. F. O. Costa, S. M. Dubiel, M. Reissner, and W. Steiner, *J. Magn. Magn. Mater.* **321**, 2160 (2009).

⁷J. Cieślak, M. Reissner, S. M. Dubiel, J. Wernisch, and W. Steiner, *J. Alloys Compd.* **460**, 20 (2008).

⁸E. A. Turov and M. P. Petrov, *Nuclear Magnetic Resonance in*

Ferro- and Antiferromagnets (Halsed Press, New York, 1972).

⁹A. P. Guimarães, *Magnetism and Magnetic Resonance in Solids* (Wiley, New York, 1998).

¹⁰W. G. Clark, M. E. Hanson, F. Lefloch, and P. Ségransan, *Rev. Sci. Instrum.* **66**, 2453 (1995).

¹¹J. S. Lord and P. C. Riedi, *Meas. Sci. Technol.* **6**, 149 (1995).

¹²T. J. Bastow and A. Trinchi, *Solid State Nucl. Magn. Reson.* **35**, 25 (2009).

¹³H. Lütgemeier and S. M. Dubiel, *J. Magn. Magn. Mater.* **28**, 277 (1982).

¹⁴I. Mirebeau, G. Parette, and J. W. Cable, *J. Phys. F: Met. Phys.* **17**, 191 (1987).

¹⁵B. Drittler, N. Stefanou, S. Bluegel, R. Zeller, and P. H. Dederichs, *Phys. Rev. B* **40**, 8203 (1989).